Identification of a key residue in K_v 7.1 potassium channel essential for sensing external potassium ions

Wenying Wang,¹ Maria Cristina Perez Flores,¹ Choong-Ryoul Sihn,¹ Hyo Jeong Kim,¹ Yinuo Zhang,² Karen J. Doyle,¹ Nipavan Chiamvimonvat,^{2,3} Xiao-Dong Zhang,² and Ebenezer N. Yamoah¹

 K_v 7.1 voltage-gated K^+ (K_v) channels are present in the apical membranes of marginal cells of the stria vascularis of the inner ear, where they mediate K^+ efflux into the scala media (cochlear duct) of the cochlea. As such, they are exposed to the K^+ -rich (\sim 150 mM of external K^+ (K^+_e)) environment of the endolymph. Previous studies have shown that K_v 7.1 currents are substantially suppressed by high K^+_e (independent of the effects of altering the electrochemical gradient). However, the molecular basis for this inhibition, which is believed to involve stabilization of an inactivated state, remains unclear. Using sequence alignment of S5-pore linkers of several K_v channels, we identified a key residue, E290, found in only a few K_v channels including K_v 7.1. We used substituted cysteine accessibility methods and patch-clamp analysis to provide evidence that the ability of K_v 7.1 to sense K^+_e depends on E290, and that the charge at this position is essential for K_v 7.1's K^+_e sensitivity. We propose that K_v 7.1 may use this feedback mechanism to maintain the magnitude of the endocochlear potential, which boosts the driving force to generate the receptor potential of hair cells. The implications of our findings transcend the auditory system; mutations at this position also result in long QT syndrome in the heart.

INTRODUCTION

K_v7.1 (KCNQ1 or KvLQT1) voltage-gated K⁺ (K_v) channel is encoded by the KCNQ1 gene. Mutations in the KCNQ1 gene have been shown to lead to long QT syndrome (LQTS), a hereditary condition associated with life-threatening cardiac arrhythmias (Wang et al., 1996; Splawski et al., 2000; Tester et al., 2005). K_v7.1 channels also play critical roles in the inner ear, where they mediate K⁺ flux across the apical membrane of the marginal cells (MCs) of the stria vascularis into the scala media of the cochlear duct (Wangemann, 2002). The flux of K⁺ across cells of the stria vascularis and the high input impedance of a 15-nm interstrial space establish the endocochlear potential, which enhances hair-cell generator potential by approximately twofold (Salt et al., 1987; Nin et al., 2008). K₇7.1 has been shown to be prominently expressed in MCs of the stria vascularis (Wangemann, 2002). Null or missense mutations of K_v7.1 result in hearing loss (Schmitt et al., 2000; Casimiro et al., 2004; Maljevic et al., 2008). In the cochlear duct, K_v7.1 is

exposed to \sim 150 mM of external K⁺ (K⁺_e), imposing an unfavorable chemical gradient for the flux of K⁺ from MCs into the scala media (Salt et al., 1987; Nin et al., 2008).

Previous studies have shown that K_v7.1 currents were suppressed substantially by increased K⁺_e (Larsen et al., 2011). A plausible mechanism is that K⁺_e stabilizes an inactivated state of the channel; however, the molecular basis remains unknown. Here, we aimed to address the molecular basis of the regulation of $K_v7.1$ by K_e^+ . We identified a negatively charged amino acid residue, glutamate at position 290 (E290), located in the S5-pore linker of human K_v7.1 (hK_v7.1), as a potential regulatory site by K⁺_e. Neutralization of the negatively charged amino acid by cysteine (C) substitution (E290C) significantly decreased the effects of K_e. We further demonstrated that modification of E290C by negatively charged MTS reagents restored the sensitivity of K_v7.1 to K_e^+ , supporting the essential role of the negative charge at this position in sensing K⁺_e. Our findings provide molecular insights into the modulation of K_v7.1 by K⁺_e. Regulation of K_v7.1 by K⁺_e may allow the precise control of the extent of K+ flux across the apical membrane

Correspondence to Ebenezer Yamoah: enyamoah@gmail.com; or Xiao-Dong Zhang: xdzhang@ucdavis.edu Dr. Kim died on 17 June 2014.

Abbreviations used in this paper: CHO, Chinese hamster ovary; GHK, Goldman–Hodgkin–Katz; hK $_{\rm v}$, human voltage-gated K $^{+}$; K $_{\rm e}$, external K $^{+}$; K $_{\rm v}$, voltage-gated K $^{+}$; LQTS, long QT syndrome; MC, marginal cell; MTSEA, 2-aminoethyl MTS; MTSES, 2-sulfonatoethyl MTS; MTSET, 2-(trimethylammonium) ethyl MTS; MTSPeS, 5-sulfonatopentyl MTS.

© 2015 Wang et al. This article is distributed under the terms of an Attribution–Noncommercial–Share Alike–No Mirror Sites license for the first six months after the publication date (see http://www.rupress.org/terms). After six months it is available under a Creative Commons License (Attribution–Noncommercial–Share Alike 3.0 Unported license, as described at http://creativecommons.org/licenses/by-nc-sa/3.0/).

Downloaded from http://rupress.org/jgp/article-pdf/145/3/201/1794395/jgp_201411280.pdf by guest on 03 December 2025

¹Department of Physiology, School of Medicine, University of Nevada, Reno, Reno, NV 89557

²Department of Internal Medicine, Division of Cardiovascular Medicine, School of Medicine, University of California, Davis, Davis, CA 95616

³Department of Veterans Affairs, Northern California Health Care System, Mather, CA 95655

of MCs to regulate the magnitude of the endocochlear potential.

MATERIALS AND METHODS

Isolation of mouse stria vascularis

The study was performed in accordance with the guidelines of the Institutional Animal Care and Use Committee of the University of Nevada, Reno. Postnatal day 12–14 C57BL/6J mice were used for the study. The animals were killed, and the temporal bones were removed and placed in saline solution containing (mM): 90 NaCl, 50 lactobionic acid, 5 KCl, 10 HEPES, 1.2 MgCl₂, 1.13 Ca²⁺ lactobionate, and 5 p-glucose, pH 7.4 with NaOH. The stria vascularis was identified and carefully dissected using fine forceps. The stria vascularis was digested with 1 mg/ml protease type XXIV at 37°C for 10 min. The tissue was transferred to saline solution containing 1 mg/ml bovine serum albumin and 20 µg/ml DNase I for 3 min. The semi-intact epithelia preparation was then washed, placed on a slide, and anchored in the recording chamber, which was mounted on the stage of an inverted microscope (BX50W1; Olympus).

Generation of mutant forms of hK_v7.1 channels

WT hK_v7.1 clone (GenBank accession no. AF000571) (Sharma et al., 2004) was subcloned into a pIRES2-EGFP plasmid vector (Takara Bio Inc.). Single-point amino acid substitution at the E290 position into K (lysine), A (alanine), C (cysteine), and D (aspartic acid), and single-point amino acid substitution at E284,

D286, and E295 positions into C were generated using a Quick-Change II mutagenesis kit (Agilent Technologies) and verified by automated sequencing.

Cell culture and transfection of hK_v7.1

Chinese hamster ovary (CHO) cell line was used to express the hK_v7.1 WT and mutant (MT) channels. CHO cells were maintained in F-12 media with 10% FBS and 1× antibiotic–antimycotic mixture (Invitrogen) at 37°C with 5% CO₂. CHO cells were plated onto 12-mm coverslips in F-12 plus 10% FBS without antibiotics and cultured 12–24 h before transfection. Cells were transfected with the hK_v7.1-WT or hK_v7.1-MT plasmids (200 ng/well) using Lipofectamine 2000 (Invitrogen). For cotransfection of K_v7.1 or E290C with KCNE1, we used a 2:1 quantitative ratio to control the stoichiometry of the assembled channels, as reported recently (Plant et al., 2014). However, the transfection with a 2:1 ratio of DNA of KCNQ1/KCNE1 does not necessarily mean that there will be a 2:1 ratio of KCNQ/KCNE1 subunits in the functional channel.

Patch-clamp recordings

Whole-cell current recordings in MCs and CHO cells were performed using an Axopatch 200B amplifier, Digidata 1332 digitizer, and pClamp 8 software (Molecular Devices). All the recordings were performed at room temperature. The series resistance was compensated by $\sim 90\%$ during the recordings. A stock solution of linopirdine, chromanol 293B, and niflumic acid was made in 0.3 M DMSO and stored at -80°C. Current traces

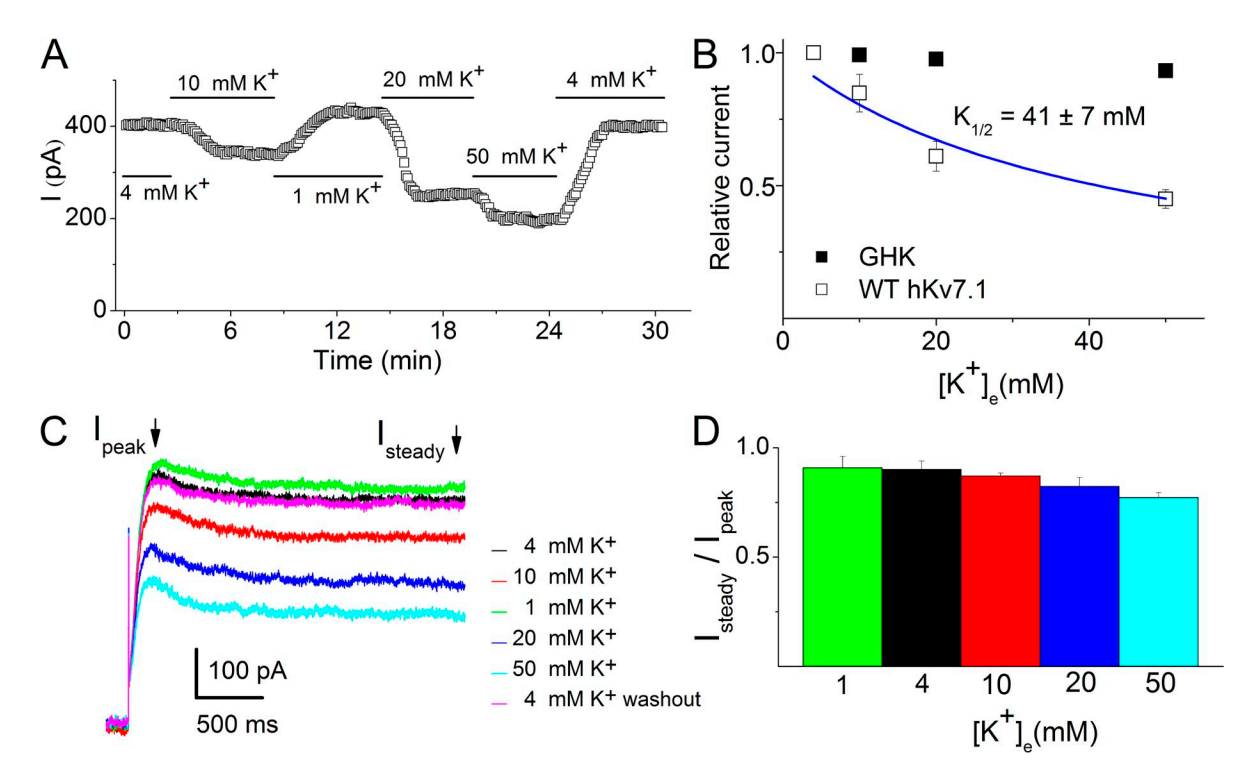


Figure 1. Inhibition of $hK_v7.1$ current by K^+_c . (A) Concentration-dependent inhibition of $hK_v7.1$ currents by K^+_c . Cells were held at -70 mV and stepped to 40 mV to activate the current. The time course of a 30-min recording of the current magnitude as the $[K^+]_c$ was continuously altered as shown. The effects of K^+_c were reversible. (B) The relationship between the relative magnitude of the $hK_v7.1$ current and $[K^+]_c$. The relative currents were calculated by normalizing the currents at different K^+_c to the current obtained at 4 mM K^+_c at the test potential of 40 mV. The experimental data (\Box , n=7) were at odds with the current magnitude predicted by the GHK equation (\blacksquare). $K_{1/2}$ of the current inhibition of 41 ± 7 mM was obtained by fitting the data points, as shown by the blue curve using a Langmüir function as described in Materials and methods. (C) Representative current traces with varied K^+_c . (D) Ratios of the steady state (I_{steady}) to the peak current (I_{peak}) density at the test potential of 40 mV using different K^+_c (n=11).

were generated using a family of voltage steps from -90 to 60 mV (10-mV increments) for 1.5 or 2.5 s, followed by a step pulse to either -30 or -80 mV from a holding potential of -70 mV. The reversal potential of the K⁺ current was determined in each experiment using an instantaneous tail current protocol elicited from a holding potential of -70 mV by applying a prepulse of 40 mV for 1.5 s before stepping to a family of test potentials from -110 to -10 mV (10-mV increments) and analyzing the resulting deactivation currents.

For MC recordings, patch electrodes contained (mM): 140 K⁺-gluconate, 5 KCl, 0.1 CaCl₂, 10 HEPES, 5 EGTA, and 5 K₂ATP, pH 7.2 with KOH. The external bath solution was constantly perfused (2–3 ml/min) and contained (mM): 90 NaCl, 50 lactobionic acid, 0–150 KCl, 1.13 Ca²⁺ lactobionate, 1.2 MgCl₂, 0.1 niflumic acid, 10 HEPES, and 10 p-glucose, pH 7.4 with NaOH. In some experiments, the K⁺_e ranged from 0 (no K⁺ added in external solution) to 150 mM. To vary K⁺ concentrations, Na⁺ was exchanged 1:1 for K⁺.

Recordings from CHO cells were performed using patch pipettes with solution consisting of (mM): 145 KCl, 0.1 CaCl₂, 2 MgCl₂, 1 EGTA, 5 K₂ATP, 0.5 GTP, and 10 HEPES, pH 7.4 with KOH. The external bath solution was constantly perfused (2–3 ml/min) and contained (mM): 145 NaCl, 1–50 KCl, 1.8 CaCl₂, 0.5 MgCl₂, 5 D-glucose, and 10 HEPES, pH 7.4 with NaOH. To vary K⁺ concentrations, Na⁺ was exchanged 1:1 for K⁺.

MTS modifications

The stock solution of MTS reagents (Toronto Research Chemicals) was prepared in distilled water (0.3 M) and stored at $-80^{\circ}\mathrm{C}$. Aliquots of the stock solution were kept at $\sim\!1\text{--}2^{\circ}\mathrm{C}$ on ice, and the working solution containing 1 mM of the MTS reagents was reconstituted immediately before use. The reconstituted solution was discarded if not used within 5 min. Additionally, the thawed stock solution was discarded at the end of the day. DTT stock solution (0.5 M, stored at $-20^{\circ}\mathrm{C}$) was thawed and diluted to 5 mM in bath solution immediately before use.

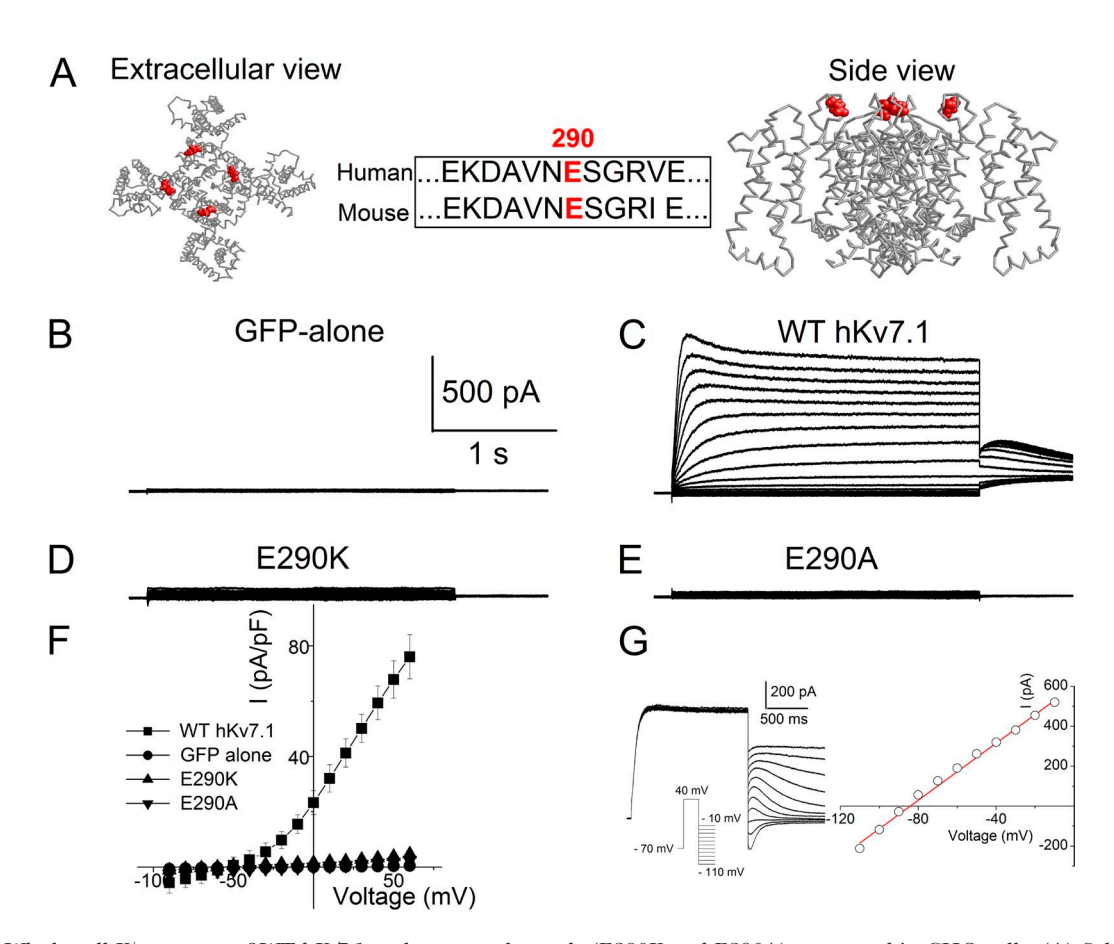


Figure 2. Whole-cell K^+ currents of WT $hK_v7.1$ and mutant channels (E290K and E290A) expressed in CHO cells. (A) Schematic diagram of the structure model of $K_v7.1$ in the open state (Smith et al., 2007), showing the residue E290 in red. Amino acid sequence alignment from residues 284–295 between human and mouse $K_v7.1$ is shown in the middle. The E290 is located in the external S5-pore linker. (B) Green fluorescence protein (GFP)-alone transfected cells did not yield measurable currents. (C) Examples of K^+ current traces recorded from CHO cells after 24–48 h of transfection with WT $hK_v7.1$ elicited from a holding potential of -70 mV using a family of test pulses ranging from -90 to 60 mV for 2.5 s with a 10-mV increment followed by a voltage step to -30 mV. (D and E) Neither E290K nor E290A yielded measurable current after 24–96 h of transfection using the pulse protocol described in C. The point mutations converted residue 290 from negative to positive and nonpolar neutral amino acids, respectively. (F) The corresponding current density-voltage relationships (n = 17). The averaged current density from the last 50 ms of the test pulse was used. (G) The reversal potential of the K^+ current was determined in each experiment using an instantaneous tail current protocol elicited from a holding potential of -70 mV by applying a prepulse of 40 mV for 1.5 s before stepping to a family of test potentials from -110 to -10 mV (10-mV increments) and analyzing the resulting deactivation currents. The current and voltage-clamp protocol (inset) are shown on the left and the corresponding instantaneous current-voltage relationship is shown on the right for 4 mM K_c^+ .

Data analysis

Curve fits and data analyses were performed using Origin software (MicroCal, LLC). We used the Goldman–Hodgkin–Katz (GHK) equation to calculate the expected current magnitude, given an internal $K^{\scriptscriptstyle +}$ concentration of 145 mM and varying $K^{\scriptscriptstyle +}_{\rm c}$ as outlined (Larsen et al., 2011). The ratio of the currents resulting from the two different $K^{\scriptscriptstyle +}_{\rm c}$ can be estimated by the GHK equation as follows:

$$I_{1}/I_{2} = (K_{i}^{C1} - K_{o}^{C1} exp(-VF/RT))/(K_{i}^{C2} - K_{o}^{C2} exp(-VF/RT)),$$
(1)

where I_1 and I_2 represent the K^+ currents generated in two different configurations of K^+ concentrations (C1, C2) across the cell membrane, $K_i^{\rm C1}/K_o^{\rm C1}$ and $K_i^{\rm C2}/K_o^{\rm C2}$; K_i and K_o represent K^+ concentrations inside and outside, respectively; V is the membrane potential; F is Faraday's number; R is the gas constant; and T is the absolute temperature.

The steady-state current of WT hK_v7.1 at 40 mV in the presence of certain concentrations of K_e^+ was normalized to that of 1 or 4 mM K_e^+ to demonstrate the relationship between the relative magnitude of the hK_v7.1 current and K_e^+ concentration ([K⁺]_e). The normalized current, which represents the unblocked fraction (*FUB*), was fitted to a Langmüir function as follows:

$$FUB = 1/(1 + [K^{+}]_{c}/K_{1/2}),$$
 (2)

where $K_{1/2}$ is the $[K^{\!+}]_e$ that effectively blocks 50% of the recorded current.

The steady-state activation curves were fitted with a one-state Boltzmann function. Where appropriate, we presented data in the form of mean \pm SD. Significant differences between groups were tested using paired/unpaired Student's t test.

RESULTS

Inhibition of K_v7.1 currents by K⁺_e

As demonstrated previously in expressed hK_v7.1 in *Xenopus laevis* oocytes (Larsen et al., 2011), the application of different concentrations of K_e^+ to hK_v7.1 channels expressed in CHO cells yielded K_e^+ current whose magnitude was highly sensitive to K_e^+ in a manner that could not be reconciled with the GHK prediction (Fig. 1, A–C). The blue line in Fig. 1 B represents the fit of hK_v7.1 current by a Langmüir function. $K_{1/2}$ was calculated to be 41 ± 7 mM (n = 7).

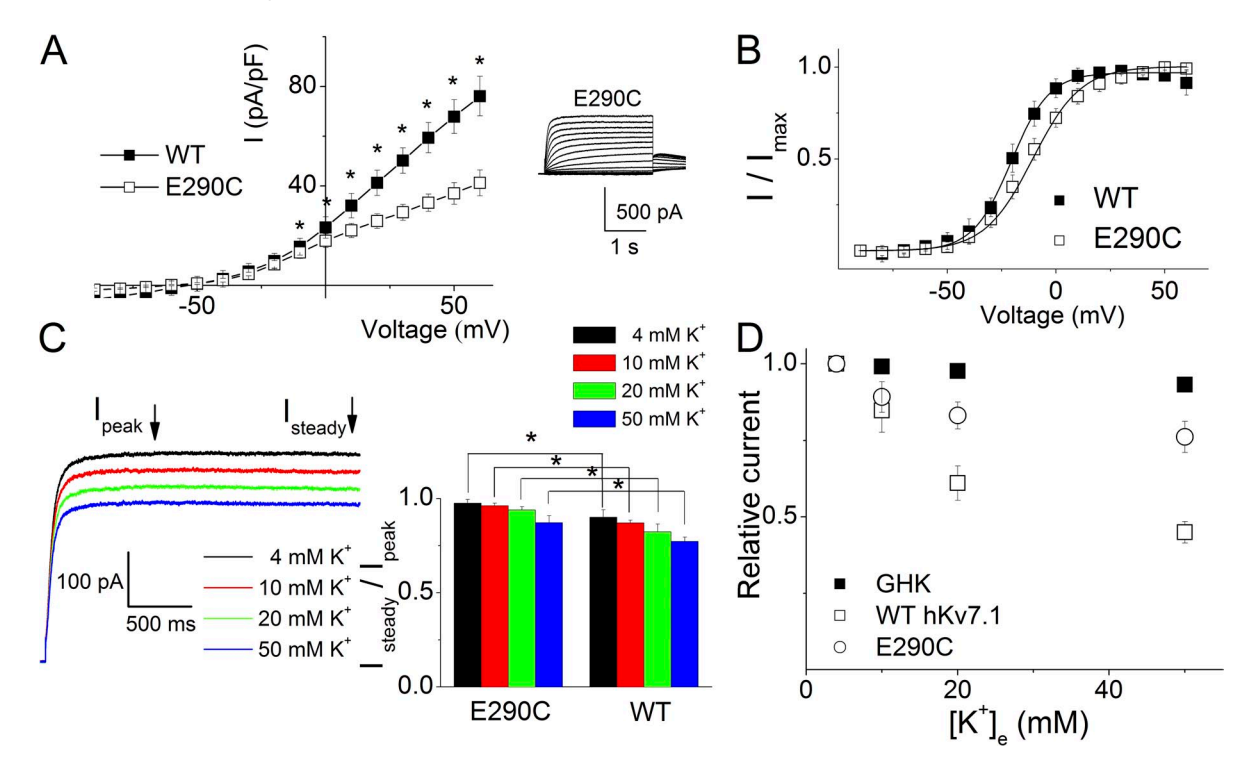


Figure 3. The E290C mutant channel yielded measurable current with less sensitivity to K_e^+ compared with WT hK_v 7.1. (A) Current density-voltage relationships of the whole-cell currents from WT hK_v 7.1 and E290C mutant channel (n=13). The averaged current density from the last 50 ms of the test pulse was used. The outward current density of E290C was significantly smaller than that of WT channels (*, P < 0.05). Representative current traces of E290C are shown in the inset on the right. (B) Steady-state voltage-dependent activation of WT and E290C channels. The tail currents immediately after stepping to −30 mV were normalized to the largest tail current and plotted against the preceding prepulse voltages. The midpoint of activation ($V_{1/2}$ in mV) and the slope factors (k) of the activation curves obtained from WT and E290C channels are −20.4 ± 1.9 and 9.2 ± 1.1 for WT hK_v 7.1 (n=11) and −13.3 ± 0.8 and 11 ± 1.2 for E290C (n=9), respectively. (C) Representative current traces (left) of E290C with varied K_e^+ . The ratios of the steady state to the peak current density at 40 mV are shown on the right. The ratios are significantly larger than that of WT channels (*, P < 0.05). (D) The relationship between the relative magnitude of the E290C current and K_e^+ . The experimental data (O, n=7) were approaching the predicted current magnitude (I) by the GHK equation. This is in contrast to the WT hK_v 7.1 channels (I), which were at odds with predicted values by the GHK equation.

To further assess the extent of the apparent K_e^+ -mediated inactivation, we measured the ratio of the amplitude of the steady state to the peak whole-cell K^+ current as illustrated in Fig. 1 D. There was an enhanced inactivation by the increased K_e^+ .

Identification of a potential amino acid residue in $K_v7.1$ for sensing the K_e^+

A variety of hK_v channels have been reported to respond disparately toward elevated $K^{+}_{\rm e}.$ For example, besides the expected current magnitude reduction as predicted by the GHK equation, hK_v1.5 and hK_v4.3 are insensitive to increasing $K^{+}_{\rm e}$ (Larsen et al., 2011). In contrast, K_v11.1 activity is exquisitely sensitive to changes in $K^{+}_{\rm e}$ (Sanguinetti et al., 1995). The extracellular loops of K_v7.1 consist of several negatively charged amino acid residues. We focused on subtle changes in the sequence of the S5-pore linker among members of the K_v channels. Amino acid sequence alignment of S5-pore linkers of K_v1.5, K_v4.3, and K_v7.1 revealed three negatively charged amino acids at equivalent positions at 284, 286,

and 295. Moreover, K_v 7.1 is endowed with an additional negatively charged amino acid at position 290 (E290), making the residue unique (Fig. 2 A, middle). The extracellular location of E290 shown in Fig. 2 A (left and right) is based on a structural model of the transmembrane domain of K_v 7.1 and the open-state crystal structure of K_v 1.2 (Smith et al., 2007).

The negative charge at 290 or equivalent position is only found in $K_v7.1$, its related member $K_v7.3$, as well as in $K_v10.1$ and $K_v10.2$ (EAG channels) among all the K_v channels. It is not found in $K_v1.5$ and $K_v4.3$, which are insensitive to increasing K_e^+ . Therefore, we hypothesize that E290 may serve as a sensor for K_e^+ . Indeed, a point mutation, E290K, in $hK_v7.1$ has been shown to be linked to LQTS in patients (Tester et al., 2005), although information as to whether these patients had hearing loss is unavailable.

To address the molecular basis of K_e^+ -mediated current reduction, we generated the previously reported LQTS mutant (E290K) as well as a point mutation of E290 to a neutral amino acid alanine (E290A). CHO cells transfected with green fluorescence protein only were used as

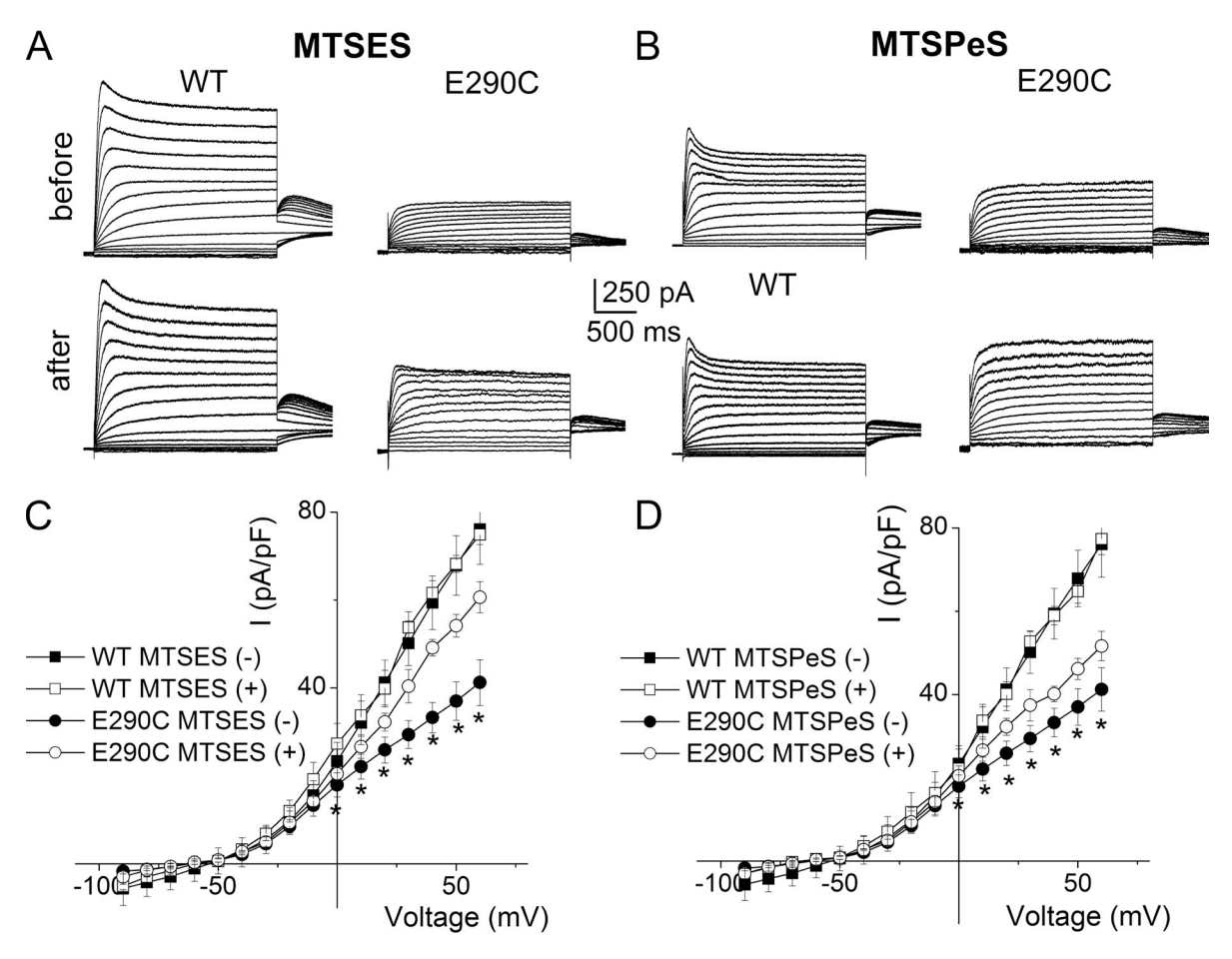


Figure 4. Modifications of E290C by negatively charged MTS reagents increased the current. (A and B) MTSES and MTSPeS modifications of WT hK $_{v}$ 7.1 (left) and E290C (right) with 4 mM K $_{v}$ 6. MTSES and MTSPeS modifications increased the E290C current but had no appreciable effects on the WT current. (C and D) The current density–voltage relationships of WT and E290C before and after MTSES (C, n = 11) and MTSPeS (D, n = 12) modifications. The outward current density was significantly increased by MTSES and MTSPeS modifications in E290C (*, P < 0.05). The averaged current density from the last 50 ms of the test pulse was used.

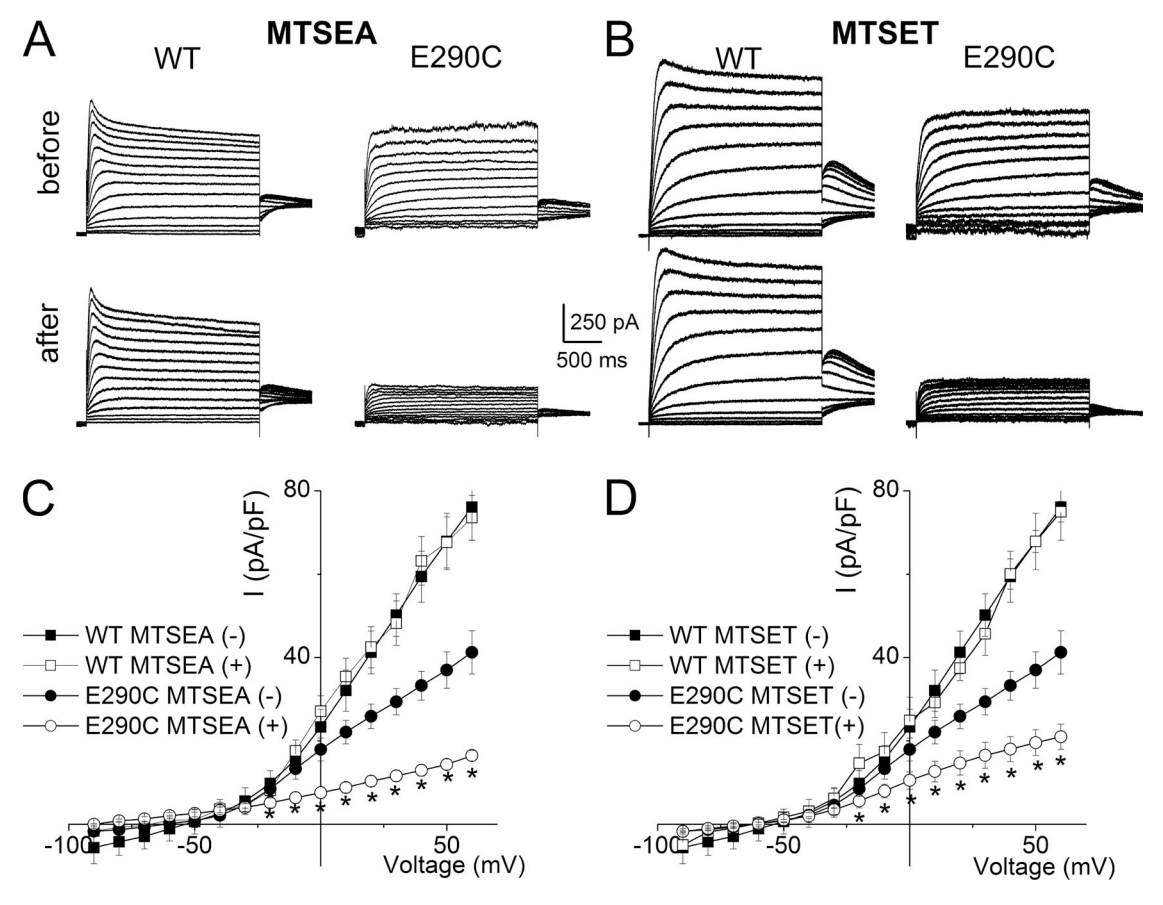


Figure 5. Modifications of E290C by positively charged MTS reagents decreased the current. (A and B) MTSEA and MTSET modifications of WT hK,7.1 (left) and E290C (right) with 4 mM K+c. MTSEA and MTSET modifications decreased the E290C current but had no appreciable effects on the WT current. (C and D) The current density-voltage relationship of WT and E290C before and after MTSEA (C, n = 7) and MTSET (D, n = 9) modifications. The outward current density was significantly reduced by MTSEA and MTSET modifications (*, P < 0.05). The averaged current density from the last 50 ms of the test pulse was used.

controls (Fig. 2 B). No measurable outward currents were detected in CHO cells transfected with either E290K or E290A (Fig. 2, D-F) compared with WT channel (Fig. 2 C). Our data supported E290K as the pathogenic disease-causing variant in LQTS patients.

We have also used the instantaneous tail current protocol to further assess the reversal potential of WT K_v7.1 current. As shown in Fig. 2 G using 4 mM K⁺_e, the current reversed at -84 mV, close to the calculated K+ equilibrium potential (E_K) of -91 mV.

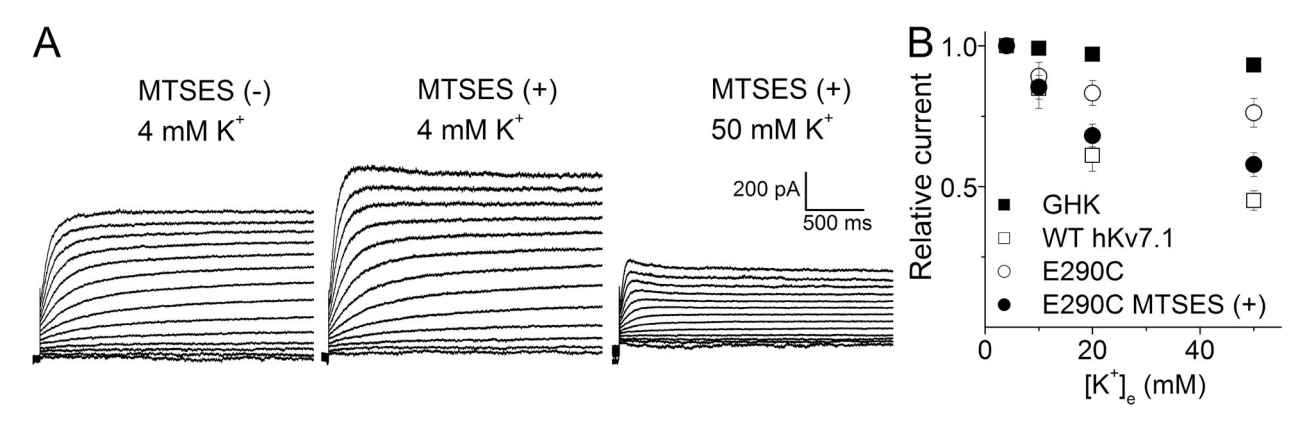


Figure 6. Modification of E290C by MTSES restored its sensitivity to K⁺_e. (A) Current traces recorded in 4 mM K⁺_e before (left) and after (middle) MTSES modification. The right panel shows the current traces after perfusion by 50 mM K⁺_e after MTSES modification. (B) The comparison of the K⁺_e sensitivities of WT, E290C, and MTSES-modified E290C. Note that after modification by MTSES, data obtained from E290C (\bullet , n = 5) were approaching the WT values (\square).

The effect of K_{e}^{+} on E290C current approximated the values predicted by the GHK equation

Mutating E290 to cysteine (C) in hK_v7.1 (E290C) gave rise to a functional channel, albeit with a significantly reduced current magnitude compared with the WT current (Fig. 3 A). The steady-state half-activation voltage (V_{1/2}) of the E290C current was shifted by \sim 7 mV to the right compared with that of the WT channel (Fig. 3 B). Increased K⁺_e decreased the E290C current (Fig. 3 C, left); however, the ratio of the steady state to the peak currents (Fig. 3 C, right) was significantly increased compared with that of the WT channels, showing a reduced apparent inactivation in the E290C current. Moreover, the effect of K⁺_e on E290C current approximated the values predicted by the GHK equation (Fig. 3 D). The data from the WT channel were replotted in Fig. 3 D for comparison.

The essential role of the negative charge at the 290 position of $K_{\nu}7.1$ in sensing $K^{+}_{\rm e}$ revealed by MTS modifications

We further hypothesize that restoration of the negative charge at E290C may increase the current amplitude and K_e sensitivity. Therefore, we modified the E290C mutant channel using the negatively charged MTS compound, 2-sulfonatoethyl MTS (MTSES). Modification of E290C by MTSES increased the magnitude of the current, as shown in Fig. 4 (A and C). In contrast, the positively charged MTS reagent 2-aminoethyl MTS (MTSEA) had the opposite effects on the current magnitude (Fig. 5, A and C). To confirm the role of the negative charge at position 290, we used another negatively charged 5-sulfonatopentyl MTS (MTSPeS) and positively charged 2-(trimethylammonium) ethyl MTS (MTSET) to modify E290C and observed similar patterns for the current alteration (Fig. 4, B and D, for MTSPeS and Fig. 5, B and D, for MTSET, respectively).

None of these MTS reagents had any appreciable effects on the WT channels (Figs. 4 and 5).

We reasoned that if indeed the negatively charged residue at position 290 is responsible for $K^{\scriptscriptstyle +}_{\rm e}$ -mediated current reduction with increasing $K^{\scriptscriptstyle +}_{\rm e}$ concentrations, modification of E290C by negatively charged MTSES may restore the $K^{\scriptscriptstyle +}_{\rm e}$ sensitivity. Fig. 6 A shows the E290C current before (left) and after (middle) MTSES modifications. The right panel further shows the $K^{\scriptscriptstyle +}_{\rm e}$ effects (50 mM) on the MTSES-modified E290C. The sensitivity of the MTSES-modified E290C to $K^{\scriptscriptstyle +}_{\rm e}$ approximated that of the WT channel, as shown in Fig. 6 B. These findings suggested that the negative charge at the 290 position is essential for channel function and for the sensing of $K^{\scriptscriptstyle +}_{\rm e}$.

Effects of K_e^+ on E284C, D286C, and E295C K_v 7.1 mutant channels were similar to the WT channels

To further test the unique role of the negative charge at the 290 position (E290), we constructed three additional point mutations by neutralizing the negative charges of E284, D286, and E295 located in the S5-pore linker of K_v 7.1 to cysteine (C). As stated early, these three negatively charged amino acids are not unique to K_v 7.1 and are also present in the S5-pore linkers of K_v 1.5 and K_v 4.3. The effects of K_e^+ 0 on E284C, D286C, and E295C are shown in Fig. 7. As demonstrated in the relationships between the relative current magnitude and the K_e^+ 1, the experimental data of K_e^+ 2 on the three mutant channels were nearly superimposable on that of the WT channels. They were all at odds with predicted values by the GHK equation (Fig. 7 B).

Modifications of E284C, D286C, and E295C mutant channels by MTS reagents did not alter the current profile Similar experiments as performed for the WT channel and E290C in Figs. 4 and 5 were performed to test the

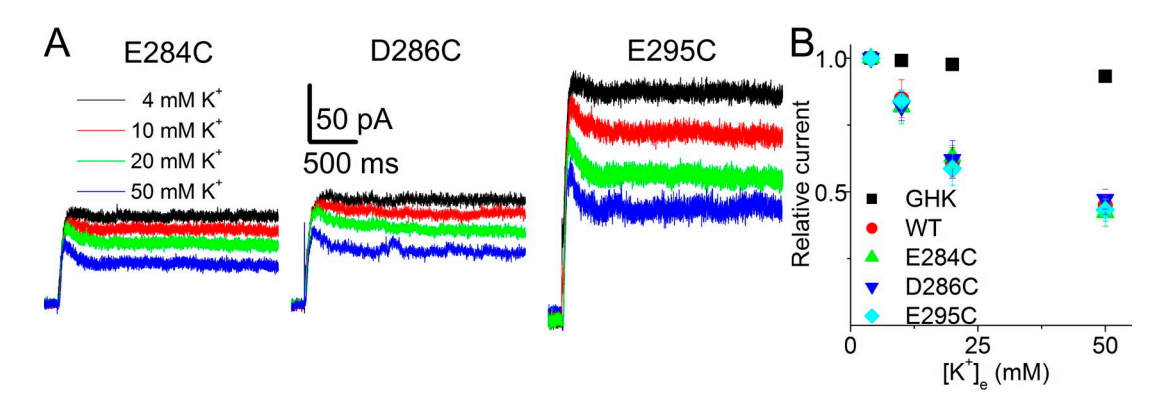


Figure 7. Functional expression and K_e^+ inhibition of E284C, D286C, and E295C currents. (A) Representative current traces of E284C, D286C, and E295C with different K_e^+ . The currents were recorded after 48–96 h of transfection using the pulse protocol described in Fig. 2 C. (B) The relationships between the relative current magnitude and the K_e^+ of E284C (n = 8), D286C (n = 6), and E295C (n = 6). The experimental data of the three mutant channels were nearly superimposable on the WT hK_v7.1 data. They were all at odds with predicted values by the GHK equation.

effects of MTSES and MTSEA modification on E284C, D286C, and E295C mutant channels (Fig. 8). The current density–voltage relationships of the three mutants before and after MTSES or MTSEA are shown in Fig. 8 (C and D, respectively). The outward current density was not significantly altered by MTSES and MTSEA modification for all three mutants.

Effects of K_e^+ on K^+ current generated by $K_v7.1$ and KCNE1

The endogenous K_v7.1 channels in MCs may be assembled by K_v7.1 and KCNE1 (minK) subunits. To further test the mechanism of K⁺_e effects on the assembled K_v7.1 channels, we coexpressed WT hK_v7.1/KCNE1 and E290C/KCNE1 in CHO cells to examine the mutational and MTSES modification effects on the channel function, as shown in Fig. 9. Fig. 9 A shows the WT hK_v7.1/KCNE1 currents before and after MTSES modification. The bottom panel shows the time course of the current resulting from the MTSES modification followed by the application of DTT at 40 mV. The change in current amplitude of E290C/KCNE1 by MTSES modification is shown in Fig. 9 B. The increase in current amplitude from MTSES modification was reversed by DTT, as shown in the bottom panel. The ratios of the current

before and after MTSES modification are shown in Fig. 9 C. We observed a significant increase in current magnitude of the E290C/KCNE1 channel after MTSES modification, similar to the E290C channel expressed alone, as shown in Fig. 4 (A and C). The sensitivity of the channels to K⁺_e was further tested for the WT hK_v7.1/KCNE1 and MTSES-modified E290C/KCNE1 channels, as shown in Fig. 9 (D and E). Higher [K⁺]_e results in the reduction of current for the WT hK_v7.1/KCNE1 channel reminiscent of the WT hK_v7.1 channel. Moreover, MTSES modification of E290C/KCNE1 channel restores the K⁺_e sensitivity comparable to that of WT K_v7.1/KCNE1, as shown in Fig. 9 F.

$\ensuremath{\mathrm{K^+_e}}\xspace\text{-}\xspace$ induced reduction of the currents in the MCs of the inner ear

K_v7.1 channels have been identified at the apical membrane of MCs and are presumed to be the main channel responsible for the efflux of K⁺ from MCs into the scala media in the inner ear (Wangemann, 2002; Nin et al., 2008). Indeed, null or missense mutations in K_v7.1 result in profound hearing loss as well as LQTS, as seen in Jervell and Lange-Nielsen syndrome (Jervell and Lange-Nielsen, 1957; Barhanin et al., 1996; Zheng et al., 1999; Johnson et al., 2000; Casimiro et al., 2004).

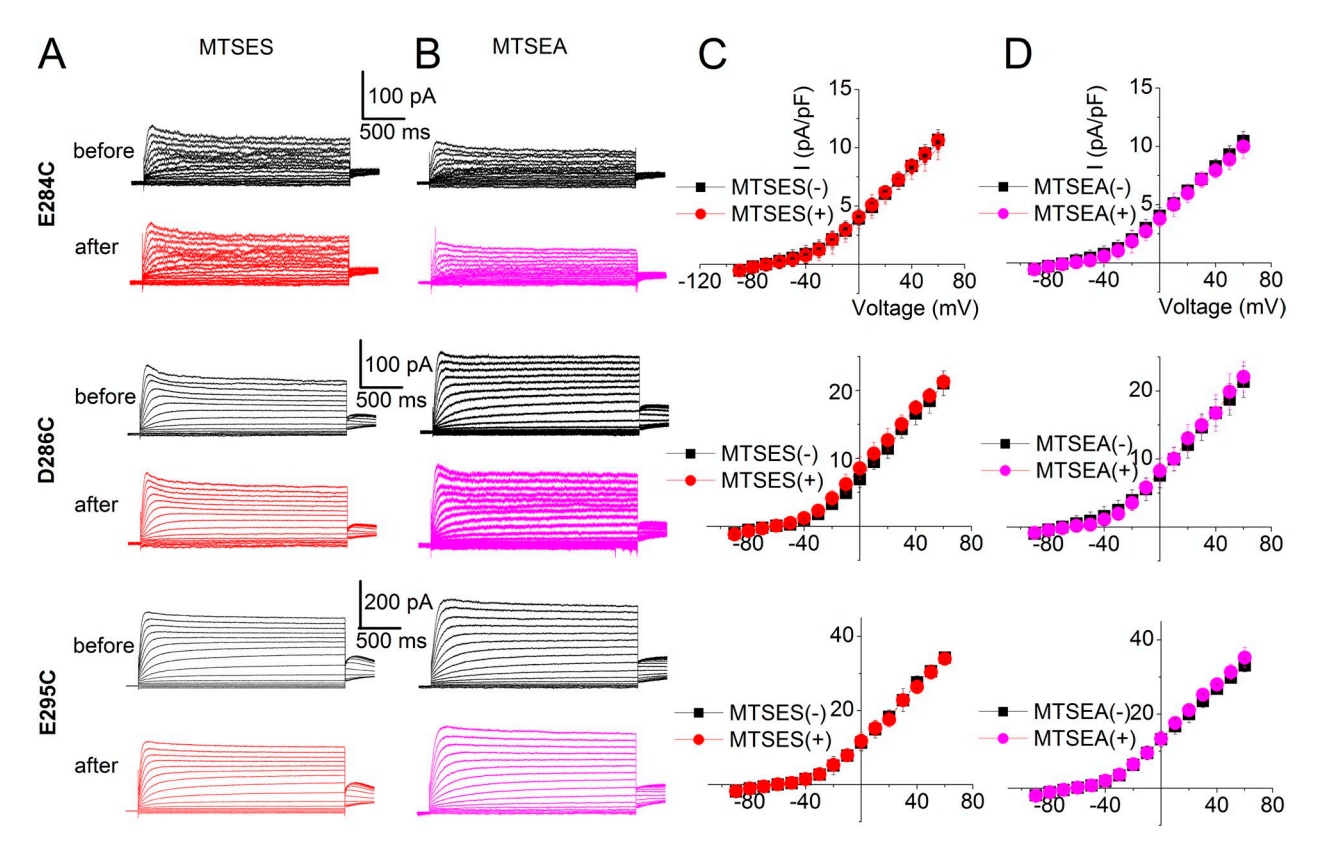


Figure 8. Modifications of E284C, D286C, and E295C by charged MTS reagents did not alter the current. (A and B) MTSES and MTSEA modifications of the three mutant channels. (C and D) The current density-voltage relationships of the three mutant channels before and after MTSES (C, n = 6, 5, and 5 for E284C, D286C, and E295C, respectively) and MTSEA (D, n = 5 for each mutant) modifications. The outward current density was not significantly altered by MTSES and MTSEA modification for all three mutants. The averaged current density from the last 50 ms of the test pulse was used.

To this end, we directly tested the effects of K⁺_e on the whole-cell K+ currents recorded from MCs in an intact strip of stria vascularis, as shown in Fig. 10 (A-C). The recorded current using 5.4 mM K⁺_e was found to be sensitive to linopirdine (Fig. 10 E), a known blocker of K_v7 channels (Leão et al., 2009; Anderson et al., 2013). The half-blocking concentration is $4.25 \pm 0.06 \,\mu\text{M}$ (n = 5). To validate that the major portion of the current was mediated by K_v7.1, we tested the sensitivity of the current to a specific K_v7.1 blocker, chromanol 293B (Fig. 10 F), a known blocker of the K_v7.1 channel (Robbins, 2001; Lerche et al., 2007; Anderson et al., 2013). There was a dose-dependent inhibition of the current by chromanol 293B (Fig. 10 G). Collectively, the data suggest that the majority of the whole-cell K⁺ currents in MCs are mediated by K_v7.1. More importantly, the K_v7.1-mediated currents from MCs were inhibited by the increased K⁺_e, as shown in Fig. 10 (A-C). Using the GHK equation, we calculated the current magnitude at 40 mV and compared it with the experimental data (Fig. 10 D). The currents from the GHK prediction were at odds with the experimental data, in line with the hetero-expressed hK_v7.1 channel shown in Fig. 1 B.

DISCUSSION

The endolymph of the inner ear is unique compared with other extracellular fluid in its high K^+ concentration. This paper provides a molecular account of the handling of K_e^+ by Kv7.1. In the cochlear duct where K_v 7.1 channels in MCs are exposed to the endolymph, which consists of \sim 150 mM K_e^+ , it would be exertemely important in K_e^+ regulation. High K_e^+ -induced current reduction in K_v 7.1 has been reported (Larsen et al., 2011), suggesting that the K_e^+ stabilizes an inactivated state in K_v 7.1 channels. However, the molecular basis remains unknown.

Functional roles of E290 in the S5-pore linker of $K_{\nu}7.1$ in $K^{+}_{\,\,\mathrm{e}}$ inhibition of the channel

Previous reports have identified the turret region of the outer mouth of the S5-pore linker as an important regulator of inactivation of the *Shaker* K^+ channel (Schönherr and Heinemann, 1996). Compared with the EAG-related family of K^+ channels, e.g., $K_v11.1$, there are significant differences in the S5-pore linker in that

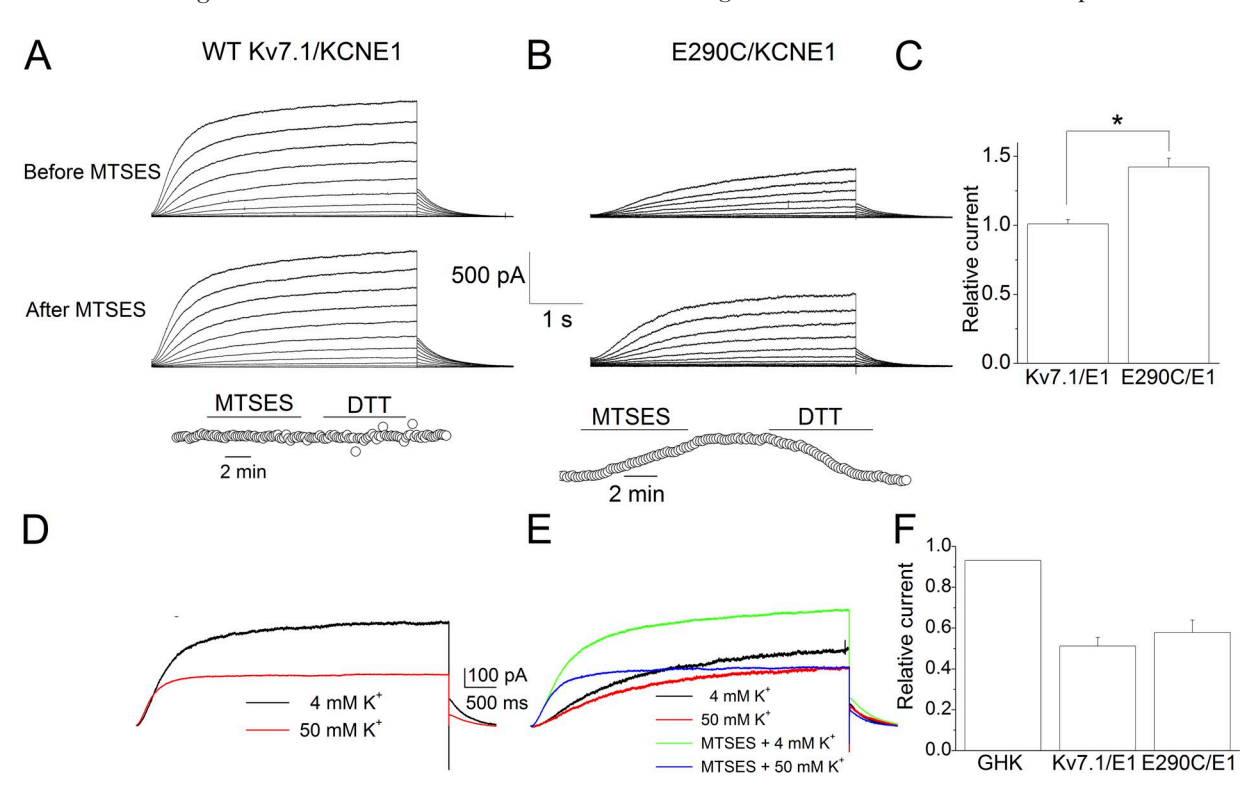


Figure 9. Modifications of E290C/KCNE1 by MTSES approximated the WT $K_v7.1/KCNE1$ current phenotype. (A and B) Current traces of WT $K_v7.1/KCNE1$ and E290C/KCNE1 before and after MTSES modification. The bottom panel shows the time course of the current resulting from the MTSES modification and DTT application at a test pulse of 40 mV. The increase in current amplitude from MTSES modification was reversed by DTT. (C) Summary data for the effects of MTSES modification on WT $K_v7.1/KCNE1$ compared with E290C/KCNE1 channels. The relative current was calculated by normalizing the current at 40 mV after MTSES modification to that before MTSES modification (n = 9 for E290C/KCNE1 and n = 5 for WT $K_v7.1/KCNE1$; *, P < 0.05). (D) The effects of 50 mM K_v^* on the WT $K_v7.1/KCNE1$ current. (E) The reduction of the E290C/KCNE1 current by 50 mM K_v^* before and after MTSES modification. (F) The reduction of the E290C/KCNE1 current by 50 mM K_v^* after MTSES modification approximated that of the WT $K_v7.1/KCNE1$ current. The relative current was calculated by normalizing the current obtained using 50 mM K_v^* to that at 4 mM K_v^* at the test potential of 40 mV (n = 5 for WT $K_v7.1/KCNE1$ and n = 7 for E290C/KCNE1).

the $K_v11.1$ has a much longer linker between the outer helix of the pore domain and the pore helix, consisting of \sim 40 residues, as opposed to 12–15 residues in other members of the K_v channels (Liu et al., 2002; Torres et al., 2003). We focused on subtle changes in the sequence of the S5-pore linker among members of the K_v channels. We identified a key residue, E290, which is located at the extracellular S5-pore linker of $K_v7.1$, to be essential for sensing K_e^+ . However, we cannot rule out the possibility that other residues may also be important in sensing K_e^+ .

The outcomes of MTS modifications of E290C provide additional evidence to implicate the negative charge at position 290 as the key regulator in K^+_e -mediated current reduction. It is possible that the binding and neutralization of the negatively charged residue E290 by K^+_e produce a conformational change that leads to a slower transition rate from the inactivated state of the channel, as suggested by a previous study demonstrating that K^+_e stabilizes an inactivated state in $K_{\nu}7.1$ channels (Larsen et al., 2011). Our cysteine-scanning mutagenesis study supports the notion that E290 is accessible from the extracellular side of the channels, thus

allowing binding to the K^+ ions. Moreover, neutralization of the negative charge by cysteine substitution results in a decrease of the outward current, consistent with increased propensity of the channels in the inactivated state. An alternative possibility for the current reduction by high K^+_e is the direct binding of K^+ ions to the negatively charged residue, leading to the block of the channels. This second possibility remains unlikely based on the results of the previous study (Larsen et al., 2011).

Our findings are in keeping with previous reports, but they are in contrast with reports showing that coexpression of K_v 7.1 and KCNE1 in *Xenopus* oocytes suffices to eliminate K^+_e -mediated reduction of the I_{Ks} (Larsen et al., 2011). One likely possibility for the disparate findings may result from the use of different expression systems. *Xenopus* oocytes have endogenous KCNE1 and overexpression of the β relative to the α subunit can yield markedly different biophysical outcomes (Seebohm et al., 2001). In our study, the molar ratio for K_v 7.1/KCNE1 was calculated based on the recently reported stoichiometry of 2:1 (Plant et al., 2014), reducing potential artifacts emanating from heterologous expression systems.

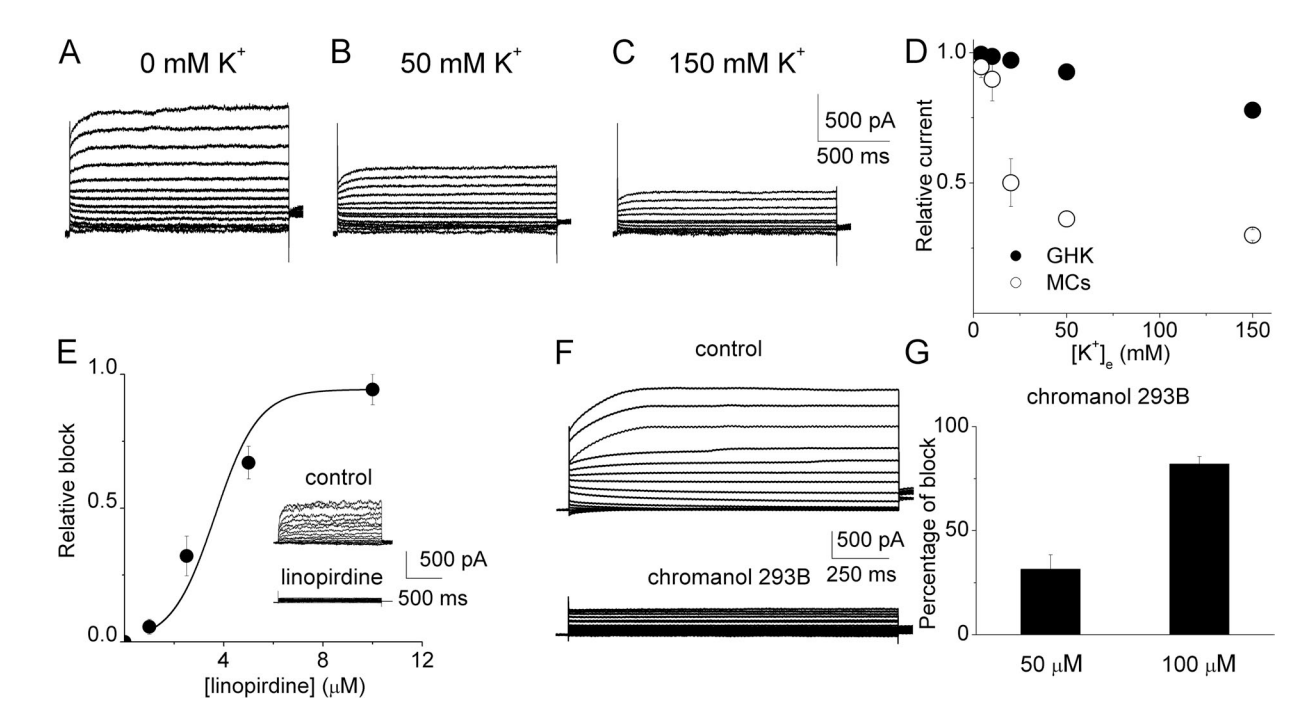


Figure 10. Inhibition of the linopirdine- and chromanol 293B–sensitive currents in MCs of the stria vascularis by K_e^+ . (A–C) Representative whole-cell outward current recordings from MCs under conditions when Cl^- current was suppressed with 100 μM niflumic acid and when K_e^+ was increased from 0 to 150 mM. Currents were elicited from a holding potential of -70 mV using a family of voltage steps ranging from -90 to 60 mV for 1.5 s with a 10-mV increment, followed by a voltage step to -20 mV. (D) The current reduction resulting from the increased K_e^+ in comparison with the prediction by the GHK equation. The relative currents were calculated by normalizing the currents at different K_e^+ to the current obtained at 1 mM K_e^+ at the test potential of 40 mV. The relative currents obtained (n=8) were significantly smaller than the predicted values when K_e^+ is 20, 50, or 150 mM. (E) Dose-dependent inhibition of the outward currents from MCs by linopirdine at the test potential of 40 mV. The half-inhibition concentration was 4.25 ± 0.06 μM (n=5). Typical currents before and after the application of 10 μM linopirdine were shown in the inset. (F) Currents recorded from MCs in 1 mM K_e^+ before (top) and after (bottom) the application of 100 μM chromanol 293B. The same voltage protocol described in A–C was used. (G) Dose-dependent inhibition of the outward current at the test potential of 40 mV from MCs by chromanol 293B (n=7 for 50 μM; n=6 for 100 μM).

The role of K_v7.1 channels in the generation of the endocochlear potential

Assuming the resting membrane potential (V_{rest}) of hair cells of approximately -60 mV, the direct-current potential of ~140 mV ensues from the endocochlear potential (~80 mV), which generates a standing current, forming the basis for the mechanoelectrical "battery theory" of cochlear transduction (von Békésy, 1951; Salt et al., 1987; Nin et al., 2008). In contrast, in most cells, the external potential (ground) is 0 mV. Thus, nonselective cationic channels in cells rely on their V_{rest} as the electromotive force for ion influx. Previous studies have shown that the endocochlear potential is generated by the high K⁺ throughput across the apical membrane of intermediate cells into an ~15-nm high impedance space called interstrial space (Salt et al., 1987; Nin et al., 2008). Moreover, the persistent K⁺ flux across the MCs is not necessarily the generator of the endocochlear potential. The continuous flow of K⁺ in the cochlear duct is essential for normal cochlear function because it prevents K⁺ accumulation in the perilymph, curtailing sustained hair cell and neuronal membrane depolarization (Spicer and Schulte, 1998).

Possible functional roles of $K_{\rm e}^+$ inhibition of $K_{\rm v}7.1$ in MCs of the stria vascularis

K_v7.1 and KCNE1 have been localized in cells of the stria vascularis, and the current mediated by K_v7 channels has been implicated in K⁺ secretion into the endolymph (Sakagami et al., 1991; Marcus and Shen, 1994; Wangemann et al., 1996; Neyroud et al., 1997; Nicolas et al., 2001). A requirement for K_v7.1 current is further supported by the deafness and vestibular defects found in $Kcnq1^{-/-}$ and $Kcne1^{-/-}$ mice (Vetter et al., 1996; Zheng et al., 1999; Johnson et al., 2000; Casimiro et al., 2004). If K_v7.1 indeed is expressed along the apical membrane of MCs as proposed (Wangemann, 2002), the properties of the channel described in this paper would be expected to have marked physiological ramifications. In prehearing, cochlear duct K_v7.1 in MCs is likely to operate at optimum conditions (Rybak et al., 1992; McGuirt et al., 1995). As endolymph K⁺ concentration increases during inner ear development, it is predicted that a sizable number of K_v7.1 channels would be confined in the inactivated state, preventing excessive K⁺ accumulation in the endolymph. As in many biological systems, this negative feedback scenario would be an exquisite strategy to control the flow of K⁺ and maintain the endocochlear potential of the cochlear duct.

We thank members of our laboratory for comments on the manuscript.

This work was supported by grants from the National Institutes of Health (NIH; DC007592 and DC010386 to E.N. Yamoah), the NIH/National Heart, Lung, and Blood Institute (R01 HL085727 and R01 HL085844 to N. Chiamvimonvat), the VA Merit Review

Grant (I01 BX000576 to N. Chiamvimonvat), and the American Heart Association Western States Affiliate Beginning Grant-in-Aid (14BGIA18870087 to X.-D. Zhang).

The authors declare no competing financial interests.

Angus C. Nairn served as editor.

Submitted: 26 August 2014 Accepted: 27 January 2015

REFERENCES

Anderson, U.A., C. Carson, L. Johnston, S. Joshi, A.M. Gurney, and K.D. McCloskey. 2013. Functional expression of KCNQ (Kv7) channels in guinea pig bladder smooth muscle and their contribution to spontaneous activity. *Br. J. Pharmacol.* 169:1290–1304. http://dx.doi.org/10.1111/bph.12210

Barhanin, J., F. Lesage, E. Guillemare, M. Fink, M. Lazdunski, and G. Romey. 1996. K(V)LQT1 and lsK (minK) proteins associate to form the I(Ks) cardiac potassium current. *Nature*. 384:78–80. http://dx.doi.org/10.1038/384078a0

Casimiro, M.C., B.C. Knollmann, E.N. Yamoah, L. Nie, J.C. Vary Jr., S.G. Sirenko, A.E. Greene, A. Grinberg, S.P. Huang, S.N. Ebert, and K. Pfeifer. 2004. Targeted point mutagenesis of mouse Kcnq1: phenotypic analysis of mice with point mutations that cause Romano-Ward syndrome in humans. *Genomics*. 84:555–564. http://dx.doi.org/10.1016/j.ygeno.2004.06.007

Jervell, A., and F. Lange-Nielsen. 1957. Congenital deaf-mutism, functional heart disease with prolongation of the Q-T interval and sudden death. Am. Heart J. 54:59–68. http://dx.doi.org/10.1016/ 0002-8703(57)90079-0

Johnson, K.R., Q.Y. Zheng, and L.C. Erway. 2000. A major gene affecting age-related hearing loss is common to at least ten inbred strains of mice. *Genomics*. 70:171–180. http://dx.doi.org/10.1006/geno.2000.6377

Larsen, A.P., A.B. Steffensen, M. Grunnet, and S.P. Olesen. 2011. Extracellular potassium inhibits Kv7.1 potassium channels by stabilizing an inactivated state. *Biophys. J.* 101:818–827. http://dx.doi.org/10.1016/j.bpj.2011.06.034

Leão, R.N., H.M. Tan, and A. Fisahn. 2009. Kv7/KCNQ channels control action potential phasing of pyramidal neurons during hippocampal gamma oscillations in vitro. J. Neurosci. 29:13353– 13364. http://dx.doi.org/10.1523/JNEUROSCI.1463-09.2009

Lerche, C., I. Bruhova, H. Lerche, K. Steinmeyer, A.D. Wei, N. Strutz-Seebohm, F. Lang, A.E. Busch, B.S. Zhorov, and G. Seebohm. 2007. Chromanol 293B binding in KCNQ1 (Kv7.1) channels involves electrostatic interactions with a potassium ion in the selectivity filter. *Mol. Pharmacol.* 71:1503–1511. http:// dx.doi.org/10.1124/mol.106.031682

Liu, J., M. Zhang, M. Jiang, and G.N. Tseng. 2002. Structural and functional role of the extracellular s5-p linker in the HERG potassium channel. J. Gen. Physiol. 120:723–737.

Maljevic, S., T.V. Wuttke, and H. Lerche. 2008. Nervous system KV7 disorders: breakdown of a subthreshold brake. J. Physiol. 586:1791– 1801. http://dx.doi.org/10.1113/jphysiol.2008.150656

Marcus, D.C., and Z. Shen. 1994. Slowly activating voltage-dependent K⁺ conductance is apical pathway for K⁺ secretion in vestibular dark cells. *Am. J. Physiol.* 267:C857–C864.

McGuirt, J.P., R.A. Schmiedt, and B.A. Schulte. 1995. Development of cochlear potentials in the neonatal gerbil. *Hear. Res.* 84:52–60. http://dx.doi.org/10.1016/0378-5955(95)00015-V

Neyroud, N., F. Tesson, I. Denjoy, M. Leibovici, C. Donger, J. Barhanin, S. Fauré, F. Gary, P. Coumel, C. Petit, et al. 1997. A novel mutation in the potassium channel gene KVLQT1 causes

- the Jervell and Lange-Nielsen cardioauditory syndrome. *Nat. Genet.* 15:186–189. http://dx.doi.org/10.1038/ng0297-186
- Nicolas, M., D. Demêmes, A. Martin, S. Kupershmidt, and J. Barhanin. 2001. KCNQ1/KCNE1 potassium channels in mammalian vestibular dark cells. *Hear. Res.* 153:132–145. http://dx.doi.org/10.1016/S0378-5955(00)00268-9
- Nin, F., H. Hibino, K. Doi, T. Suzuki, Y. Hisa, and Y. Kurachi. 2008. The endocochlear potential depends on two K⁺ diffusion potentials and an electrical barrier in the stria vascularis of the inner ear. *Proc. Natl. Acad. Sci. USA*. 105:1751–1756. http://dx.doi.org/10.1073/pnas.0711463105
- Plant, L.D., D. Xiong, H. Dai, and S.A. Goldstein. 2014. Individual IKs channels at the surface of mammalian cells contain two KCNE1 accessory subunits. *Proc. Natl. Acad. Sci. USA*. 111:E1438–E1446. http://dx.doi.org/10.1073/pnas.1323548111
- Robbins, J. 2001. KCNQ potassium channels: physiology, pathophysiology, and pharmacology. *Pharmacol. Ther.* 90:1–19. http://dx.doi.org/10.1016/S0163-7258(01)00116-4
- Rybak, L.P., C. Whitworth, and V. Scott. 1992. Development of endocochlear potential and compound action potential in the rat. *Hear. Res.* 59:189–194. http://dx.doi.org/10.1016/0378-5955(92)90115-4
- Sakagami, M., K. Fukazawa, T. Matsunaga, H. Fujita, N. Mori, T. Takumi, H. Ohkubo, and S. Nakanishi. 1991. Cellular localization of rat Isk protein in the stria vascularis by immunohistochemical observation. *Hear. Res.* 56:168–172. http://dx.doi.org/10.1016/0378-5955(91)90166-7
- Salt, A.N., I. Melichar, and R. Thalmann. 1987. Mechanisms of endocochlear potential generation by stria vascularis. *Laryngoscope*. 97:984– 991. http://dx.doi.org/10.1288/00005537-198708000-00020
- Sanguinetti, M.C., C. Jiang, M.E. Curran, and M.T. Keating. 1995. A mechanistic link between an inherited and an acquired cardiac arrhythmia: HERG encodes the IKr potassium channel. *Cell*. 81:299–307. http://dx.doi.org/10.1016/0092-8674(95)90340-2
- Schmitt, N., M. Schwarz, A. Peretz, I. Abitbol, B. Attali, and O. Pongs. 2000. A recessive C-terminal Jervell and Lange-Nielsen mutation of the KCNQ1 channel impairs subunit assembly. *EMBO J.* 19:332–340. http://dx.doi.org/10.1093/emboj/19.3.332
- Schönherr, R., and S.H. Heinemann. 1996. Molecular determinants for activation and inactivation of HERG, a human inward rectifier potassium channel. *J. Physiol.* 493:635–642
- Seebohm, G., C. Lerche, A.E. Busch, and A. Bachmann. 2001. Dependence of I(Ks) biophysical properties on the expression system. *Pflugers Arch.* 442:891–895.
- Sharma, D., K.A. Glatter, V. Timofeyev, D. Tuteja, Z. Zhang, J. Rodriguez, D.J. Tester, R. Low, M.M. Scheinman, M.J. Ackerman, and N. Chiamvimonvat. 2004. Characterization of a KCNQ1/KVLQT1 polymorphism in Asian families with LQT2: implications

- for genetic testing. J. Mol. Cell. Cardiol. 37:79–89. http://dx.doi.org/10.1016/j.yjmcc.2004.03.015
- Smith, J.A., C.G. Vanoye, A.L. George Jr., J. Meiler, and C.R. Sanders. 2007. Structural models for the KCNQ1 voltage-gated potassium channel. *Biochemistry*. 46:14141–14152. http://dx.doi.org/ 10.1021/bi701597s
- Spicer, S.S., and B.A. Schulte. 1998. Evidence for a medial K⁺ recycling pathway from inner hair cells. *Hear. Res.* 118:1–12. http://dx.doi.org/10.1016/S0378-5955(98)00006-9
- Splawski, I., J. Shen, K.W. Timothy, M.H. Lehmann, S. Priori, J.L. Robinson, A.J. Moss, P.J. Schwartz, J.A. Towbin, G.M. Vincent, and M.T. Keating. 2000. Spectrum of mutations in long-QT syndrome genes. KVLQT1, HERG, SCN5A, KCNE1, and KCNE2. Circulation. 102:1178–1185. http://dx.doi.org/10.1161/01.CIR.102.10.1178
- Tester, D.J., M.L. Will, C.M. Haglund, and M.J. Ackerman. 2005. Compendium of cardiac channel mutations in 541 consecutive unrelated patients referred for long QT syndrome genetic testing. *Heart Rhythm.* 2:507–517. http://dx.doi.org/10.1016/j.hrthm.2005.01.020
- Torres, A.M., P.S. Bansal, M. Sunde, C.E. Clarke, J.A. Bursill, D.J. Smith, A. Bauskin, S.N. Breit, T.J. Campbell, P.F. Alewood, et al. 2003. Structure of the HERG K⁺ channel S5P extracellular linker: Role of an amphipathic alpha-helix in C-type inactivation. *J. Biol. Chem.* 278:42136–42148.
- Vetter, D.E., J.R. Mann, P. Wangemann, J. Liu, K.J. McLaughlin, F. Lesage, D.C. Marcus, M. Lazdunski, S.F. Heinemann, and J. Barhanin. 1996. Inner ear defects induced by null mutation of the isk gene. *Neuron.* 17:1251–1264. http://dx.doi.org/10.1016/S0896-6273(00)80255-X
- von Békésy, G. 1951. D.C. potentials and energy balance of the cochlear partition. *J. Acoust. Soc. Am.* 23:576–582. http://dx.doi.org/10.1121/1.1906807
- Wang, Q., M.E. Curran, I. Splawski, T.C. Burn, J.M. Millholland, T.J. VanRaay, J. Shen, K.W. Timothy, G.M. Vincent, T. de Jager, et al. 1996. Positional cloning of a novel potassium channel gene: KVLQT1 mutations cause cardiac arrhythmias. *Nat. Genet.* 12:17– 23. http://dx.doi.org/10.1038/ng0196-17
- Wangemann, P. 2002. K⁺ cycling and the endocochlear potential. *Hear. Res.* 165:1–9. http://dx.doi.org/10.1016/S0378-5955(02)00279-4
- Wangemann, P., Z. Shen, and J. Liu. 1996. K⁺-induced stimulation of K⁺ secretion involves activation of the IsK channel in vestibular dark cells. *Hear. Res.* 100:201–210. http://dx.doi.org/10.1016/0378-5955(96)00127-X
- Zheng, Q.Y., K.R. Johnson, and L.C. Erway. 1999. Assessment of hearing in 80 inbred strains of mice by ABR threshold analyses. *Hear. Res.* 130:94–107. http://dx.doi.org/10.1016/S0378-5955 (99)00003-9